Poly(lactic acid)/Polystyrene Bioblends Characterized by Thermogravimetric Analysis, Differential Scanning Calorimetry, and Photoacoustic Infrared Spectroscopy

Abdellatif Mohamed,[1] Sherald H. Gordon,[2] Girma Biresaw[1]

[1]*Cereal Products and Food Science Unit, National Center for Agricultural Utilization Research, Agricultural Research Service, United States Department of Agriculture, Peoria, Illinois 61604*
[2]*Plant Polymer Research Unit, National Center for Agricultural Utilization Research, Agricultural Research Service, United States Department of Agriculture, Peoria, Illinois 61604*

Received 25 October 2006; accepted 12 April 2007
DOI 10.1002/app.26783
Published online 17 July 2007 in Wiley InterScience (www.interscience.wiley.com).

ABSTRACT: Bioblends are composites of at least one biodegradable polymer with nonbiodegradable polymer. Successful development of bioblends requires that the biodegradable polymers be compatible with other component polymers. Compatibility can be assessed by evaluating the intermolecular interactions between the component polymers. In this work, the interaction in binary bioblends comprising biodegradable poly(lactic acid) (PLA) and polystyrene (PS) was investigated using thermogravimetric analysis (TGA), differential scanning calorimetry (DSC), and Fourier transform infrared photoacoustic spectroscopy (FTIR-PAS). The TGA studies indicated that incorporation of PLA in PS resulted in thermal destabilization of PS. The DSC studies showed that some parameters favored partial miscibility of PS in PLA, while others favored immiscibility, such as the existence of two glass transitions. The FTIR-PAS spectra revealed the presence of intermolecular n–π interactions between PLA and PS and indicated that the degree of interaction was dependent on the concentrations of the polymers in the bioblends. FTIR-PAS results computed via differential spectral deconvolution were consistent with, and therefore support, the results of TGA and DSC analyses of PLA/PS bioblends. The degradation kinetics, used to determine the degradation mechanism, revealed a two- or three-step mechanism. © 2007 Wiley Periodicals, Inc. J Appl Polym Sci 106: 1689–1696, 2007

Key words: bioblends; poly(lactic acid); polystyrene; TGA; DSC; FTIR-PAS; n–π bond interaction; kinetics

INTRODUCTION

Poly(lactic acid) (PLA) is one of many synthetic biodegradable polymers[1,2] that include, polycaprolactone (PCL), and poly(hyroxybutyrate-co-hydroxyvalerate) (PHBHV).[2] Blends of these biodegradable polymers with various materials are being studied for a variety of industrial applications. For product development, synthetic biodegradable polymers have been blended with natural polymers, nonbiodegradable synthetic polymers, compatiblizers,[3] plasticizers,[4–6] salts,[7] and other synthetic biodegradable polymers. Natural polymers that have been blended with synthetic biodegradable polymers for research and product development include starch,[8,9] cellulose,[9] lignin,[10] gluten,[11] and dextran.[12,13]

Polymer blends containing at least one biodegradable polymer component are referred to as bioblends. Currently, bioblends are being developed for such uses as (a) materials packaging[4–9]; (b) drug delivery systems; and (c) bioabsorbable sutures[14] and tissue transplantation.[15] The development of useful products from blends of synthetic biodegradable polymers requires that they be compatible with the materials with which they are blended. Compatibility is related to the physical and chemical properties of the polymers being blended, as well as the blending parameters (e.g., temperature, pressure, humidity, shear, etc.).[16–19] Although no quantitative models exist at present for predicting blend compatibility from component properties and blending parameters, a variety of methods exist that are being used to assess the degree of compatibility of blends. These methods can be broadly categorized into interfacial, thermal, mechanical, morphological, spectroscopic, and scattering techniques.[16–19]

To increase understanding of compatibility in blends containing synthetic biodegradable polymers, studies on model bioblends were done at this laboratory. These were binary blends in which one component was the synthetic biodegradable polymer,

Names are necessary to report factually on available data; however, the USDA neither guarantees nor warrants the standard of the product, and the use of the name by the USDA implies no approval of the product to the exclusion of others that may also be suitable.

Correspondence to: A. Mohamed (mohameda@ncaur.usda.gov).

Journal of Applied Polymer Science, Vol. 106, 1689–1696 (2007)

poly(lactic acid) (PLA), and the second component was the non-biodegradable polymer polystyrene (PS). The ultimate goal was to apply improved understanding of compatibility in PLA/PS bioblends toward the development of predictive models for compatibility of bioblends containing other synthetic biodegradable polymers.

In previous studies, various properties of model bioblends such as interfacial tension,[20–22] interfacial adhesion,[23] and tensile properties[24] were examined. Fourier transform infrared photoacoustic spectroscopy (FTIR-PAS), which is a nondestructive method that allows probing the molecular level interactions between the polymers in solid binary blends,[25–33] is well suited for analysis of noncovalent molecular interactions in extruded poly(lactic acid)/polystyrene blends. In this work, FTIR-PAS was applied to experimentally establish the existence of molecular interactions in blends of PLA with PS, and to corroborate the interactions with thermodynamic evidence from thermogravimetric analysis (TGA) and differential scanning calorimetry (DSC) of the PLA/PS bioblends.

EXPERIMENTAL

Polymer blend preparation

Polymers investigated in this work were obtained from commercial sources and were used as received. D,L-poly(lactic acid) abbreviated (PLA) was donated by Gargil and Polystyrene (Styron 685D, Minneapolis, MN) abbreviated (PS) was obtained from Dow (Dow Research Center, Detroit, MI). Binary blends of PLA with PS were prepared by manually mixing the corresponding pellets. The composition of the blends ranged from pure (neat) PLA to pure (neat) PS, in 25% (w/w) intervals; 75 : 25, 50 : 50, and 25 : 75. The mathematical modeling for T_g temperature prediction was done on the three above-mentioned ratios plus two additional blends, 85 : 15 and 35 : 65. Compounding of blends was accomplished by melt extrusion into ribbons on a ZSK-30 twin screw extruder (Werner & Pfleiderer, Ramsey, NJ). The ribbons exiting the extruder were converted into pellets using a Bronco II mechanical chopper (Killion, Cedar Grove, NJ), or manually after the extrusion was completed. Details of the extrusion procedure were given earlier.[24]

Thermogravimetric analysis

TGA measurements were taken using a TGA 2050 Thermogravimetric Analyzer (TA Instruments, New Castle, DE). First, samples were ground into powder using a Brinkmann/Retsch high-speed shaker mill. To avoid heat degradation for the duration of milling, samples were immersed in liquid nitrogen for 2–3 s. Samples (~ 10 mg) were heated from room temperature to 800°C using 10°C/min and held at an isotherm for 3 min. The TGA data were plotted as temperature versus weight %, from which onset and final decomposition temperatures were obtained. (Hereafter, these plots will be referred to as TGA plots.) The TGA data were also plotted as temperature versus derivative of weight %, from which peak decomposition temperatures were obtained. (Hereafter, these plots will be referred to as DTGA plots.)

TGA was also used to determine the degradation kinetics of neat PLA or PS and blends. Three heating rates, 10, 15, and 20°C/min, were used to calculate the activation energy of degradation (E_a) according to Flynn and Wall[34] based on the following eq. (1)

$$\log \beta \cong 0.457\left(-\frac{E_a}{RT}\right) + \left[\log\left(\frac{AE_a}{R}\right) - \log F(a) - 2.315\right] \quad (1)$$

where β is the heating rate, T is the absolute temperature, R is the gas constant, a is the conversion, E_a is the activation energy, and A is the pre-exponential factor. According to this equation, at the same conversion, E_a can be obtained from the slope of the plot of log β versus $1000/T$ (K). The E_a was calculated by the software provided by TA Instruments. The E_a value was determined for all samples at each heating rate and the percent conversion per minute is reported.

Differential scanning calorimetry

DSC measurements were performed using a TA DSC™ 2920 (TA Instruments, New Castle, DE). As with TGA, powdered sample (~ 50 mg) was loaded in a stainless steel pan, and the pan was then sealed. Once loaded on the DSC, the sample was equilibrated at 0°C, after which the temperature increased at 10°C/min to 200°C; an isotherm was maintained for 1 min; then, the sample was cooled at 10°C/min to –70°C. For a better data fitting using the Gordon–Taylor–Woods model, two additional blends were used, PLA : PS; 85 : 15, and 35 : 65 (total of five blends).

Fourier transform infrared photoacoustic spectroscopy

Three different binary blends of PLA and PS (Table II) were tested by FTIR-PAS. The two pure (neat) polymers, PLA and PS, were tested as controls. All five samples were tested in the solid state as received with no pulverization, treatment or other sample preparation. Each pellet (~ 3-mm-thick pellets) was placed in an FTIR-PAS detector (MTEC

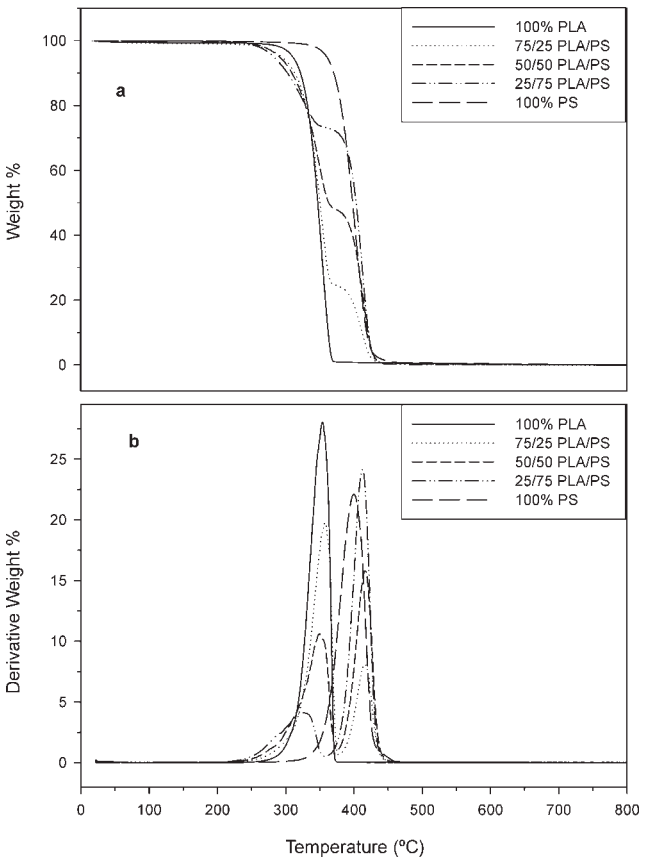

Figure 1 (a) TGA and (b) DTGA of PLA/PS bioblends.

PAS cell, Model 200, MTEC, Ames, IA) and purged with helium for ~ 15 min to maximize the photoacoustic signal-to-noise ratio. Samples were equilibrated in the PAS cell at 25°C before testing. FTIR-PAS spectra were measured using the MTEC detector on an FTS 6000 spectrometer (Digilab, Cambridge, CT) equipped with a KBr crystal beamsplitter. The light source was a water-cooled ceramic midinfrared globar delivering 150 mW energy to the sample compartment. Step-scan phase modulation at 400 Hz and $2.0\lambda_{He-Ne}$ amplitude was applied at a step rate of 2.5 Hz with software-based digital signal processing (DSP) supplied with the software (Win-IR-Pro) provided by Digilab. The 400 Hz modulation frequency probed a sampling depth of ~ 9 μm into these polymer pellets. DSP generated in-phase (0°) and quadrature (90°) components of the photoacoustic signals, which were collected at 8 cm^{-1} resolution and signal-averaged over two 1024 point scans. FTIR-PAS spectra were acquired from symmetric interferograms by correcting the phase rotation angle and ratioing the signals against a carbon black reference. Interferograms were Fourier-transformed using triangular apodization for optimum linear response.

Depth-specific phase angle spectra of the polymers were computed by three-dimensional (3D) interpolation as the root-mean-square values of the in-phase and quadrature components. 3D interpolation spectra were normalized to the phase angle at which the photoacoustic response is maximized prior to digital spectral comparison of the carbonyl bands.

RESULTS AND DISCUSSION

Thermogravimetric analysis

Neat PLA exhibited a one-step decomposition profile with a single transition temperature, as demonstrated by TGA and the derivative (DTGA) plots [Fig. 1(a,b)]. The TGA peak temperature is the temperature at the beginning point of the most weight loss, while the final is the temperature at the end of the degradation. These two points can be determined easily using the derivative graph. The profile for the neat polymers showed that the biodegradable PLA has lower thermal stability than PS, because its peak of degradation was at 352.5°C and it was completely decomposed (0% w/w char residue) at 376.2°C, while PS showed peak degradation at 412.3°C and was fully degraded at 449.2°C. It is worth mentioning that at 350°C PLA exhibited much more weight loss (57.4%) than PS (2.7%) despite the similar weight loss at 300°C for both neat polymers [Fig. 1(a)]. This indicates different degradation mechanisms due to structural difference between the two polymers. PLA is semicrystalline and PS is 100% amorphous.

The profile of the blends showed two degradation transitions representing the components of the blend. The transition that appeared at lower temperature was closer to PLA and the later one was closer to PS. The peak of the transitions representing the blend components came out at temperatures lower than those of the neat polymers they represent. This is clearly demonstrated in the DTGA plot of Figure 1(b). The blend with 25 wt % PLA (25:75 PLA:PS) showed two transitions where the first decomposition profile was similar to the neat PLA, 326.5°C for PLA in the blend versus 352.5°C for neat PLA, while the second came out at the same temperature of the neat PS (412.3°C) (Table I). Overall, PLA degradation transitions are lower when it is part of the blend,

TABLE I
TGA Peak and Final Degradation Temperature Data of the Neat PLA, PS, and the Blends

Sample name	Profile no. 1		Profile no. 2	
	Peak (°C)	Final (°C)	Peak (°C)	Final (°C)
100% PLA	353.5	376.2	Neat PLA	
75% PLA	352.5	372.4	411.3	456.8
50% PLA	347.8	372.4	414.1	456.5
25% PLA	326.5	356.3	412.3	456.8
0% PLA	Neat PS		412.3	449.2

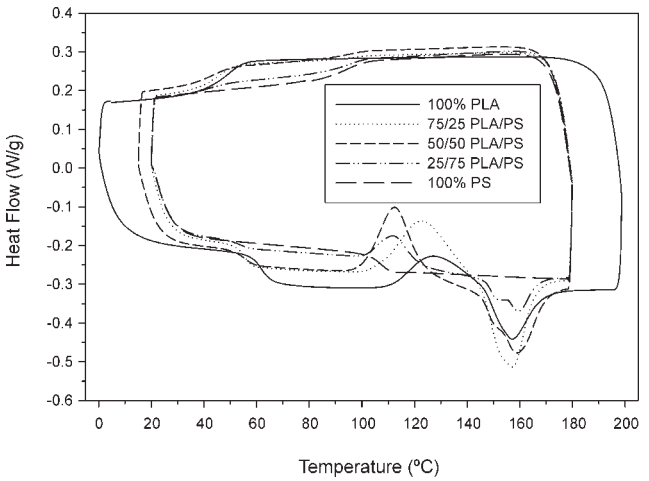

Figure 2 DSC of PLA/PS bioblends overlay.

unlike PS, where the transition came out at similar temperatures as the neat PS. This is possibly related to the effect of PS on the crystallization of PLA after extrusion and that could indicate some form of interaction between the PLA and PS during extrusion. In addition, the weight loss of the blend at 350°C relative to the neat components was very different i.e., the 100% PLA percent degradation was 57.3, 75% PLA was 49.1, 50% PLA was 38.7, 25% PLA was 26.2, and 0% PLA was 2.7 (Fig. 1). This is another way of showing the higher thermal stability of PS relative to PLA, but the magnitude of heat stability reduction is not proportional to the percent PLA in the blend. Finally, the weight loss associated with these transitions appeared to be influenced directly by the PLA content in the blend. The exact effect of these polymers on each other's degradation profile, i.e., whether the blend profile started degrading at a lower or higher temperature relative to the neat polymer, is not apparent, but phase separation was not apparent either. Although the TGA studies seem to indicate that some degree of thermal destabilization possibly occurred in some PLA/PS bioblends, this change could be an indication of some sort of interaction between PLA and PS polymers that results in unfavorable thermal stability of the blend. Since PLA is semicrystalline and PS is 100% amorphous, it is possible that the influence of PS influenced PLA crystallinity. In addition, the large difference between the T_g temperatures of the two polymers adds to the degradation mechanism.

Differential scanning calorimetry

Measurement of heat flow and temperature of transitions are ways to obtain qualitative and quantitative information about properties of various composites. Blend properties that can be predicted based on DSC measurements include degree of miscibility,[35–41] degree of intermolecular interactions,[35,41,42] and degree of crystallization.[41,43,44] As an example, the general rule for evaluating miscibility of binary blends using DSC is as follows: (a) immiscible – a blend that displays two T_g and two T_m that are composition-independent[37,41,45]; (b) miscible – a blend that displays composition-dependent single T_g and single T_m in the entire composition range,[35,37,40] (c) partially miscible – a blend that displays two T_g and two T_m that are composition-dependent,[36,39,46] and composition-dependent single T_g and single T_m in a narrow composition range.

The DSC profiles of the neat polymers and the composites are shown in Figure 2. To eliminate the thermal history of PLA and PS, all DSC data discussed below and shown in Figure 2 represent the second heating and cooling DSC cycles. Each PLA cycle included a glass transition endothermic during heating (melting) and an exothermic during cooling (crystallization) transition, while PS exhibited only glass transition (T_g). The corresponding enthalpies and heat capacity (ΔH_m, ΔH_c, and ΔC_p) and temperatures (T_m, T_c, T_{mid}) obtained from the DSC data of the neat polymers are given in Table I.

The DSC results indicate that increasing the percentage of PS in the bioblend resulted in higher T_{pm} temperature of melting, while the T_{pc} temperature has decreased at higher PS levels (Table II). That behavior was expected, because of the higher T_g of the amorphous structure of PS versus semicrystalline

TABLE II
Summary of DSC Data on Neat Polymers and Blends

	Melting temperature (T_m)			Crystallization temperature (T_c)			Glass transition temperature (T_g)			
Sample	T_o	T_p	ΔH_m[a] (J/g)	T_o	T_p	ΔH_c[a] (J/g)	T_o	T_{mid}	T_f	ΔC_{p2} (J g^{-1} °C^{-1})
100% PLA	147.0	157.2	10.4	111.6	127.0	10.0	58.5	61.8	65.2	0.460
75 : 25 PLA : PS	150.4	161.8	17.7	113.3	127.0	14.9	59.8	62.5	65.6	0.316
50 : 50 PLA : PS	151.0	163.6	12.7	113.0	124.2	12.3	55.7	60.0	67.2	0.173
25 : 75 PLA : PS	153.1	164.9	5.1	114.9	122.6	2.1	57.7	60.3	64.3	0.123
100% PS	No melting or crystallization peak						106.3	110.7	115.2	0.259

T_o, T_p, T_{mid}, and T_f indicate onset, peak, middle, and final temperatures (in °C), respectively.
[a] ΔH_m and ΔH_c indicate melting and crystallization enthalpies, respectively.

structure of PLA. The effect of blend composition on T_g is illustrated in the data (Table II), where PLA/PS bioblends displayed a reduced $T_{g\text{mid}}$ temperature as the PS content increased. This was despite the higher T_g of PS. Since glass transition is the measure of molecular mobility, lower glass transition indicates less compact PS structure in the presence of PLA. This is another indication of some form of interaction between the two polymers. The ΔH_m and ΔH_c of PLA bioblends showed a linear decrease with increasing concentration of PS (Table II). This could be used to estimate PLA and PS blend composition of unknown blend samples, because the reduction in ΔH was proportional to the amount of PS in the blend especially at the 50 and 75% PS level where the drop in ΔH was 49.5 and 75.6%, respectively. The ΔC_p of the blend decreased with increasing concentration of PS (Table II). The lower ΔC_p reflects change in the molecular size, i.e., compactness, of the blend during heating. In this case, lower ΔC_p is indicative of lower molecular size and mobility when more PS is present in the blend.

Generally, partial or complete miscibility of polymers can be measured by the presence of a single T_g or a shift in T_g.[25,26] A number of model equations were used to predict the T_g dependence of polymer blends, such as the Gordon–Taylor–Woods equation,[47] and the experimental data. The Gordon–Taylor equation is represented as follows

$$T_g^b = \frac{W_1 T_{g_1} + K W_2 T_{g_2}}{W_1 + K W_2} \quad (2)$$

where T_g^b = blends glass transition; W_1 and W_2 = weight fraction of PLA and PS, respectively; T_{g_1} and T_{g_2} = glass transition temperature of PLA and PS, respectively; and K = adjustable fitting parameter related to miscibility i.e., the strength of the interaction between the two components. The Gordon–Taylor eq. (2) can be rewritten in the following linear form where K will be the slope of the line

$$T_g^b = T_{g_1} + K\left[\frac{W_2}{W_1}(T_{g_2} - T_g^b)\right] \quad (3)$$

where $\frac{W_2}{W_1}(T_{g_2} - T_g^b) = X$, $T_g^b = Y$, and K = slope.

The value of the parameter K in eq. (3) cannot be used for completely different blend ratios.[28]

The Gordon–Taylor–Woods equation is

$$T_g^b = \frac{W_1 T_{g_1} + K(1 - W_1) T_{g_2}}{W_1 + K(1 - W_1)} \quad (4)$$

W_1 is % PLA in blend; $T_{g_1} = T_{g\text{PLA}}$, $T_{g_2} = T_{g\text{PS}}$; $T_{g\text{PS}}$ was fixed at 110.7°C. K and $T_{g\text{PLA}}$ were used as fitting parameters.

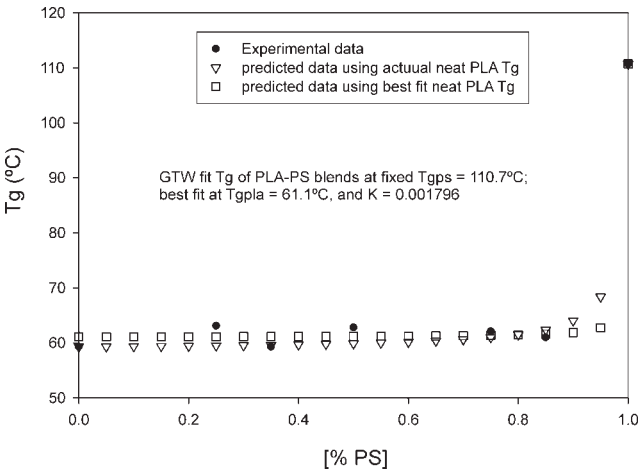

Figure 3 Experimental and predicted T_g values based on actual T_g and best fit T_g of PLA according to Gordon–Taylor–Woods.

$$T_g = \{T_{g\text{PLA}} \times (1 - [\text{PS}]) + K \times [\text{PS}] \times T_{g\text{PS}}\} / \{(1 - [\text{PS}]) + K \times [\text{PS}]\} \quad (5)$$

Three sets of data are represented in Figure 3 for the PLA/PS blends. The best fit statistically (R^2 = 0.99346) was obtained at $T_{g\text{PLA}}$ = 61.1 (compared to the measured value of 59.3), and K = 0.0018, using the experimental T_g temperature of PS (110.7°C). This is shown by the line of points (open squares) that symbolize the predicted T_g using the computed value ($T_{g\text{PLA}}$ = 61.1) that gives the best fit for the Gordon–Taylor–Woods equation. A good fit (R^2 = 0.98821), obtained at K = 0.0113, is shown by the line of points (open triangles), which represents the predicted T_g temperature of blends with different PLA/PS values using the experimental T_g temperatures, PLA (59.3°C) and PS (110.7°C). The remaining line (solid circles) corresponds to the seven experimental data points used for the equation fitting.

FTIR-PAS evidence of intermolecular interaction between PLA and PS

Figures 4 and 5 are examples of FTIR-PAS spectra of pure (neat) PLA and the 50 : 50 PLA : PS composite. The difference between the carbonyl peaks in these spectra is seen as a shift in the PLA carbonyl absorption, because PS has no significant FTIR-PAS absorbance in the carbonyl region. These spectra show the carbonyl in the blend shifted to lower wavenumber from 1767 to 1759 cm^{-1}. Such frequency shifts are considered to be definitive evidence of intermolecular interaction in polymer blends.[33] Therefore, it is proposed here that PLA interacts with PS via n–π bonding[48,49] between the unshared pair of electrons of the carbonyl groups in the PLA and the π electrons of the aromatic rings in PS. A schematic of

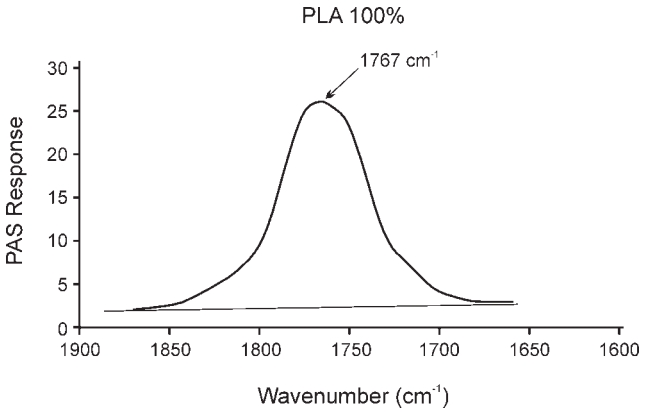

Figure 4 FTIR-PAS spectrum of carbonyl band in PLA (neat).

such interactions, depicting a possible structure of the proposed PLA : PS complex, is shown in Figure 6. Because these n–π bond complexes are relatively weaker than complexes formed via hydrogen bonds, the FTIR-PAS spectra showed relatively smaller shifts (8–11 cm^{-1}) in the positions of the carbonyl absorption bands (near 1760 cm^{-1}). The carbonyl peak shift was easily discerned by visual inspection and comparison of the overlaid spectra. Hence, the observed peak shift is definitive evidence of intermolecular polymer interaction by n–π complex formation in blends of PLA with PS.

Degradation kinetics evaluation

Equations (6)–(8) are the basis for the most published methods used for obtaining kinetics parameters from TGA analysis:

$$R = \frac{da}{dt} = K(T)f(a) \tag{6}$$

where $f(a)$ is the reaction model, a is the extend of the reaction, $K(T)$ is the temperature-dependent rate constant, ''T'' is the temperature, ''t'' is the time, and R is the degradation rate. The term $K(T)$ is assumed to obey the Arrhenius law

$$K(T) = A\exp\left(\frac{-E}{RT}\right) \tag{7}$$

where E is the activation energy, A is the pre-exponential factor, and R is the gas constant. Finally, the degradation is considered a simple nth-order reaction, which results in the following expression of the conversion dependants

$$f(a) = (1-a)^n = W^n \tag{8}$$

where n is the reaction order and W is the weight of the remaining undegraded material.

The three methods are used for single heating rates analysis or multiple heating rates. By applying Doyl's[47] approximation to the integrated form of eq. (6), we obtain the Flynn–Wall[34] eq. (9):

$$\log\beta \cong 0.457\left(\frac{-E_a}{RT}\right) + \left[\log\left(\frac{AE_a}{R}\right) - \log f(a) - 2.315\right] \tag{9}$$

The activation energy E_a can be obtained from the slope of the straight line plot of log β against $1000/T$ (K) [E_a = (slope + 0.457)R].

The TGA degradation kinetics theory is based on the fact that, the activation energy (E_a) is constant for certain level of conversion. The percent conversion versus time can be used to show the percent and temperature of conversion over time for three or more heating rates. As expected, the higher heating rate is shown to result in faster conversion.

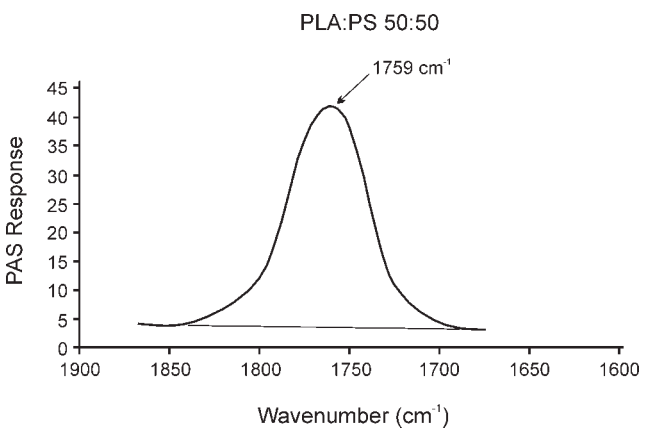

Figure 5 FTIR-PAS spectrum of carbonyl band in PLA : PS 50 : 50 blend.

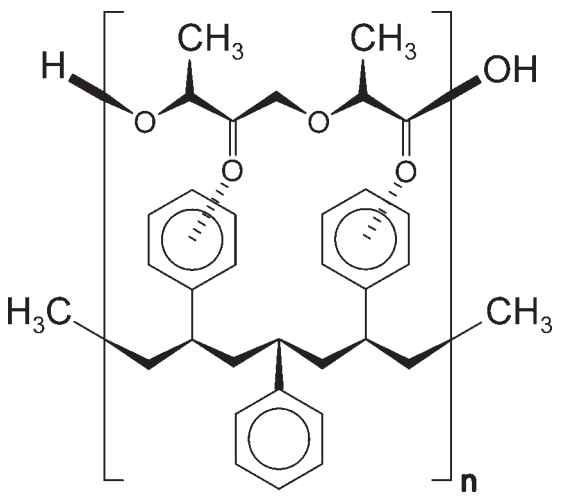

Figure 6 Complex of poly(lactic acid) and polystyrene formed by n–π bonds between carboxyl and benzyl groups.

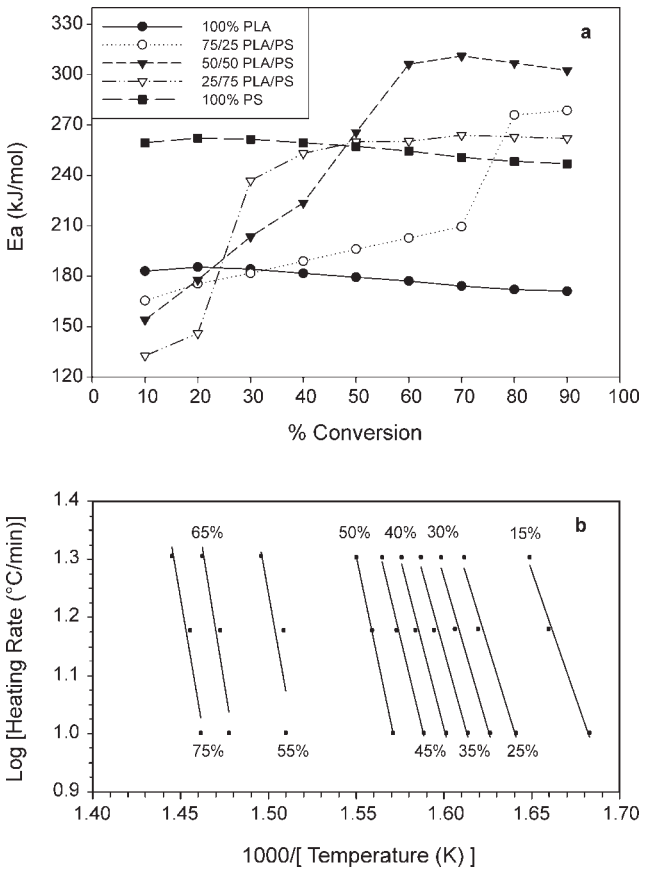

Figure 7 (a) % conversion versus E_a of the neat polymers and blends; (b) log heating rate plots of TGA kinetics analysis of 50 : 50 PLA : PS (data analyzed at 50% conversion).

All three blends showed the same phenomena of parallel lines (similar slopes) at each conversion level [Fig. 7(b)]. For each conversion, the slope of the straight line was different and represents E_a. The parallel strait lines for each % conversion [Fig. 7(b)] showed that E_a exhibited little change throughout the degradation process indicating the domination of one-step kinetic mechanism or pathway. The E_a value for the 50% conversion was used as an example, where E_a showed little change compared to other % conversions. The E_a of the blend showed values between the two neat polymers. This is consistent with the polymer interaction results derived from the above FTIR-PAS analysis results.

The plot of E_a as a function of % conversion is commonly used as an indicator for the degradation mechanism, i.e., one-step or more degradation mechanism. The straight line signifies one-step degradation mechanism, while curved line indicates more than one-step. The activation energies of PLA or PS as a function of % conversion [Fig. 7(a)] showed that PLA degraded in one-step indicating one dominant kinetics process. Although the E_a needed for the same percent conversion of the both neat polymers were different (180 J g^{-1} $^{\circ}C^{-1}$ for PLA and 260 for PS), the data indicate that structural difference between the two polymers has very little effect on the degradation mechanism. The blends' profile exhibited more than one-step of degradation, indicating the presence of more than one mechanism [Fig. 7(a)]. At a conversion level lower than 30%, the blend's degradation was dominated by E_a closer to PLA, while higher than 50% conversion was dominated by E_a similar to PS. From 30 to 50%, conversion stayed between the two neat polymers [Fig. 7(a)]. The 50% PLA blend showed E_a higher than the neat polymers. Except the blend with 25% PLA, other blends showed two-step mechanisms where the first step starts at 10% conversion and the second starts at 50% conversion [Fig. 7(a)].

CONCLUSIONS

The neat biodegradable PLA showed lower thermal stability than neat PS. TGA profiles were highly dependent on the ratio of the bioblend composition. PLA/PS bioblends showed two degradation transition temperatures, depending on the blend composition. Incorporation of PS in PLA resulted in thermal stabilization of PLA bioblends where the peak temperature of melting was increased. From the DSC data, bioblends displayed T_m and T_c values that varied with composition. This is generally considered an indication of the existence of some type of interaction between the polymers, and hence, some degree of miscibility. On the other hand, observation of another set of DSC data indicated PLA/PS immiscibility. These observations were (a) PLA/PS bioblends showed two composition independent glass transitions, and (b) PLA/PS bioblends showed ΔH_m and ΔH_c values that had a linear relation to concentration of PS. The FTIR-PAS investigation suggested the existence of n–π interactions between the biodegradable PLA and PS. The E_a value of the neat PLA was reduced by the presence of 25% PS while increased by higher PS levels, while the degradation mechanism was found to be multisteps.

We like to thank Jason Adkins for conducting the DSC and TGA experiments; Gary Gross, Brian Jasberg, Armand Loffredo, and Dick Westhoff for their help with blend extrusion; and McShell (Hairston) Clarke for technical assistance with the FTIR-PAS measurements.

References

1. Kaplan, D. L., Ed. Biopolymers from Renewable Resources; Berlin: Springer, 1998.
2. Mohanty, A. K.; Misra, M.; Hinrichsen, G. Biofibres, biodegradable polymers and biocomposites: An overview. Macromol Mater Eng 2000, 276/277(3/4), 1.

3. Wang, Y.; Hillmyer, M. Morphology and mechanical properties of polylactide (PLA)/polyethylene (PE)/PE-*b*-PLA ternary blends. Proc Polym Mater: Sci Eng 2001, 85, 597.
4. Ljungberg, N.; Andersson, T.; Wesslen, B. Film extrusion and film weldability of poly(lactic acid) plasticized with triacetine and tributyl citrate. J Appl Polym Sci 2003, 88, 3239.
5. Ljungberg, N.; Wesslen, B. The effects of plasticizers on the dynamic mechanical and thermal properties of poly(lactic acid). J Appl Polym Sci 2002, 86, 1227.
6. Ljungberg, N.; Wesslen, B. Tributyl citrate oligomers as plasticizers for poly(lactic acid): Thermo-mechanical film properties and aging. Polymer 2003, 44, 7679.
7. Soriano, I.; Evora, C. Formulation of calcium phosphates/poly (DL-lactide) blends containing gentamicin for bone implantation. J Control Release 2000, 68, 121.
8. Shogren, R. L.; Willett, J. L. Structure and properties of extruded corn starch/polymer foams. Soc Plast Eng Annu Tech Conf 2001, 59, 1860.
9. Willett, J. L.; Shogren, R. L. Processing and properties of extruded starch/polymer foams. Polymer 2002, 43, 5935.
10. Li, J.; He, Y.; Inoue, Y. Thermal and mechanical properties of biodegradable blends of poly(L-lactic acid) and lignin. Polym Int 2003, 52, 949.
11. Mohamed, A. A.; Gordon, S. H. Thermal characteristics of poly-lactic acid/wheat gluten blends. Proc NATAS Annu Conf Therm Anal Appl 2002, 30, 281.
12. Cai, Q.; Yang, J.; Bei, J.; Wang, S. A novel porous cells scaffold made of polylactide–dextran blend by combining phase-separation and particle-leaching techniques. Biomaterials 2002, 23, 4483.
13. Ouchi, T.; Kontani, T.; Ohya, Y. Modification of polylactide upon physical properties by solution-cast blends from polylactide and polylactide-grafted dextran. Polymer 2003, 44, 3927.
14. Zhang, L.; Xiong, C.; Deng, X. Biodegradable polyester blends for biomedical application. J Appl Polym Sci 1995, 56, 103.
15. Hoffman, G. T.; Soller, E. C.; McNally-Heintzelman K. M. Biodegradable synthetic polymer scaffolds for reinforcement of albumin protein solders used for laser-assisted tissue repair. Biomed Sci Instrum 2002, 3853.
16. Olabisi, O.; Robeson, L. M.; Shaw, M. T. Polymer–Polymer Miscibility; Academy Press: New York, 1979.
17. Utracki, L. A. Polymer alloys and blends; Hansen: New York, 1990.
18. Wu, S. Polymer interface and adhesion; Dekker: New York, 1982.
19. Paul, D. R.; Bucknall, C. B., Eds. Polymer Blends, Vol. 1: Formulation; Wiley: New York, 2000.
20. Biresaw, G.; Carriere, C. J. Interfacial tension of polylactic acid/polystyrene blends. J Polym Sci Part B: Polym Phys 2002, 40, 2248.
21. Biresaw, G.; Carriere, C. J. Interfacial tension of polycaprolactone/polystyrene blends by the imbedded fiber retraction method. J Appl Polym Sci 2002, 83, 3145.
22. Biresaw, G.; Carriere, C. J. Interfacial tension of eastar bio copolyester 14766/polystyrene blends. Polym Prepr (Am Chem Soc Div Polym Chem) 2002, 43, 367.
23. Biresaw, G.; Carriere, C. J.; Willett, J. L. In Proceedings of the 26th Annual Meeting of the Adhesion Society, Myrtle Beach, SC, USA, February 23–26, 2003; p 154.
24. Biresaw, G.; Carriere, C. J. Compatibility and mechanical properties of blends of polystyrene with biodegradable polyesters. Compos A 2004, 35, 313.
25. Urban, M. W.; Craver, C. D., Eds. Structure–property relations in polymers: Spectroscopy and performance. American Chemical Society: Washington DC, 1993.
26. Koenig, J. L. Fourier transform infrared spectroscopy of polymers. Adv Polym Sci 1983, 54, 87.
27. Siesler, H. W.; Holland-Moritz, K. Infrared and Raman Spectroscopy of Polymers; Marcel Dekker: New York, 1980.
28. Painter, P. C.; Coleman, M. M.; Koenig, J. L. The Theory of Vibrational Spectroscopy and Its Applications to Polymeric Materials; Wiley-Interscience: New York, 1982.
29. Drapcho, D. L.; Curbelo, R.; Jiang, E. Y.; Crocombe, R. A.; McCarthy, W. J. Digital signal processing for step-scan Fourier transform infrared photoacoustic spectroscopy. Appl Spectrosc 1997, 51, 453.
30. Jones, R. W.; McClelland, J. F. Quantitative depth profiling of layered samples using phase-modulation FT-IR photoacoustic spectroscopy. Appl Spectrosc 1996, 50, 1258.
31. Rosencwaig, A.; Gersho, A. Theory of the photoacoustic effect with solids. J Appl Phys 1976, 47, 64.
32. Vidrine, D. W. Photoacoustic Fourier transform infrared spectroscopy of solid samples. Appl Spectrosc 1980, 35, 314.
33. Koenig, J. L. Spectroscopy of Polymers, 2nd ed.; Elsevier: Amsterdam, 1999.
34. Flynn, J. H.; Wall, L. A. A quick direct method for the determination of activation energy from thermogravimetric data. Polym Lett 1966, 323.
35. Vazquez-Torres, H.; Cauich-Rodriguez, J. V.; Cruz-Ramos, C. A. Poly(vinyl alcohol)/poly(acrylic acid) blends: Miscibility studies by DSC and characterization of their thermally induced hydrogels. J Appl Polym Sci 1993, 50, 777.
36. Jang, L. W.; Lee, D. C. Polystyrene/bisphenol: A polycarbonate molecular composite by in situ polymerization. I. Preparation and characterization. Polymer 2000, 41, 1749.
37. Zheng, S.; Guo, Q.; Mi, Y. Miscibility and phase behavior in blends of phenolphthalein poly(ether sulfone) and poly(hydroxyether of bisphenol A). Polymer 2003, 44, 867.
38. Utracki, L. A. Polymer Alloys and Blends; Hansen: New York, 1990.
39. Archondouli, P. S.; Kallitsis, J. K.; Kalfoglou, N. K. Compatibilization and property characterization of polycarbonate/polyurethane polymeric alloys. J Appl Polym Sci 2003, 88, 612.
40. Krupa, I.; Luyt, A. S. Physical properties of blends of LLDPE and an oxidized paraffin wax. Polymer 2001, 42, 7285.
41. Wong, A. C.-Y.; Lam, F. Study of selected thermal characteristics of polypropylene/polyethylene binary blends using DSC and TGA. Polym Test 2002, 21, 691.
42. Urzua, M.; Gargallo, L.; Radic, D. Blends containing amphiphilic polymers. II. Poly(*N*-1-alkyl itaconamic acids) with poly(4-vinylpyridine) and poly(2-hydroxypropyl methacrylate). J Macromol Sci Phys 2000, 39, 143.
43. Ferreira, B. M. P.; Zavaglia, C. A. C.; Duek, E. A. R. Films of PLLA/PHBV: Thermal, morphological, and mechanical characterization. J Appl Polym Sci 2002, 86, 2898.
44. Lu, X.; Lim, K. Y.; Lim, F. Y.; Liu, L.; Wong, S.-C.; Zhao, J. Morphology and structures of polypropylene-aliphatic polyketone blends. Plast Rubber Compos 2002, 31, 147.
45. Manivannan, A.; Seehra, M. S. Identification and quantification of polymers in waste plastics using differential scanning calorimetry. Polym Prepr (Am Chem Soc Div Fuel Chem) 1997, 42, 1028.
46. Rao, B. M.; Rao, P. R.; Sreenivasulu, B. Polym-Plast Technol Eng 1999, 38, 311.
47. Gordon, M.; Taylor, J. S. Ideal copolymers and second order transitions of synthetic rubbers. 1. Non-crystalline copolymers. J Appl Chem. 1952, 2, 493.
48. Jang, L. W.; Lee, D. C. Polystyrene/bisphenol: A polycarbonate molecular composite by in situ polymerization. I. Preparation and characterization. Polymer 2000, 41, 1749.
49. Gardlund, Z. G. In Polymer Blends and Composites in Multiphase Systems; Han, C. D., Ed.; American Chemical Society: Washington DC, 1984; Chapter 9.